Magnetism in undoped MgO studied by density functional theory

Fenggong Wang,[1] Zhiyong Pang,[1] Liang Lin,[1] Shaojie Fang,[1] Ying Dai,[1] and Shenghao Han[1,2,][*]

[1]*School of Physics, State Key Laboratory of Crystal Materials, Shandong University, Jinan 250100, People's Republic of China*
[2]*School of Space Science and Applied Physics, Shandong University at Weihai, Weihai 264209, People's Republic of China*

The origin of magnetism in undoped MgO has been studied based on density functional theory. It is shown that Mg vacancies can induce local moments in MgO while O vacancies cannot irrespective of the concentration. The origin of the local magnetic moments comes from the partially occupied e_{g-} and t_{1u-} (or only e_{g-}) orbitals and the through-bond spin polarization mechanism mediates the ferromagnetism in MgO. For the ground state configuration of bulk MgO with two Mg vacancies, the energy difference between the ferromagnetic and antiferromagnetic states (28 meV) is smaller than the thermal energy at room temperature ($\sim$30 meV), which means that the ferromagnetic state is not stable in the bulk. For MgO thin films, Mg vacancies tend to form at the surface region because of the lower formation energy at the surface site than at the subsurface site and in the bulk. Moreover, the formation energy of Mg vacancy in MgO quantum dot decreases much, allowing a larger concentration of Mg vacancies to appear. In conclusion, the magnetism can be sustained in the quantum dot when enough holes are introduced by the large concentration of Mg vacancies. This is consistent with the experimental result of magnetism observed in MgO nanocrystals.

I. INTRODUCTION

Traditionally, considerable attention has been focused on dilute magnetic semiconductors (DMSs), in which local magnetic moments are introduced by doping elements with partially $3d$ or $4f$ subshells.[1,2] However, unexpected ferromagnetism (FM) has been observed in HfO_2 thin films without any doping.[3] This type of "d^0 ferromagnetism"[4] provides a challenge to understand the origin of the magnetism. On one hand, it is suggested that the FM in HfO_2 arises from Hf vacancies based on the results of *ab initio* electronic structure calculations.[5] On the other hand, it seems that the FM is attributed to oxygen vacancies.[6] Room temperature FM has also been found in other metal oxides such as TiO_2, In_2O_3, ZnO, CeO_2, SnO_2, and Al_2O_3, which is due to oxygen vacancies and quantum confinement effects according to the experimental results.[7,8] Moreover, theoretical calculations have suggested that the FM can be induced by cation vacancies in TiO_2, ZnO, and SnO_2,[9–13] or by anion vacancies in CeO_2.[14] Though there is a consensus that the ferromagnetism is related with native defects, considerable controversy on the origin of the magnetism still exists.

For CaO, it is indicated that a small concentration of Ca vacancies can exhibit local magnetic moments and make this nonmagnetic insulator into a half-metallic ferromagnet.[15,16] Because of the high symmetry of rock salt structure, degenerate molecular orbitals exist, and the two holes related to the Ca vacancy would occupy the molecular orbitals in a triplet state as soon as the on-site Coulomb interaction is not zero. These triplets having $3A_{2g}$ symmetry can induce short-range ferromagnetic coupling between Ca vacancies. It is also proved that spin polarization can occur at MgO surface.[17] The large magnetic moments mainly reside in surface oxygen atoms and their origin is related to the existence of $2p$ holes of well-defined spin polarization at the valence band. Recently, room temperature FM was found in MgO nanocrystalline powders prepared by sol-gel method.[18] It was ob-

served that the vacuum annealing of MgO nanocrystalline powders reduced the FM, which possibly originated from Mg vacancies at the surface of nanograins. However, the origin of magnetism in MgO is still unclear, and the question arises: why does not bulk MgO exhibit FM? In this paper, electronic and magnetic properties of MgO bulk, thin films, and quantum dot are studied by density functional theory (DFT) calculations. It is shown that Mg vacancies can induce holes and spin polarization at the top of the valence band. The formation energy of Mg vacancies decreases with the dimension of the system decreasing, allowing a larger concentration of Mg vacancies to appear in the quantum dot. Moreover, "Stoner Criterion" can be satisfied by introducing enough holes so that spontaneous ferromagnetism occurs.

II. COMPUTATIONAL METHODS

The calculations based on density functional theory[19] were performed using the projector augmented wave (PAW) method[20] and generalized gradient approximation GGA[21,22] exchange-correlation functional as implemented in VIENNA AB INITIO SIMULATION PACKAGE (VASP) code.[23,24] The valence configurations were $3s^2$ and $2s^22p^4$ for Mg and O, respectively. An energy cutoff of 400 eV was set for the plane-wave basis. For the Brillouin-zone sampling, $4 \times 4 \times 4$ Monkhorst-Pack k mesh[25] was used for the structural optimization while $11 \times 11 \times 11$ k mesh used for the density of states (DOS) calculations of MgO bulk. The convergence of the total energy with respect to the energy cutoff and the k mesh has been checked. The experimental lattice parameters:[26] $a=b=c=4.211$ Å were used for all the calculations. During the optimization, all the atoms were relaxed until the Hellman-Feynman force on each ion was less than 0.01 eV/Å.

The formation of a point defect depends on the growth or annealing conditions such as the relative abundance of the corresponding host atoms, which can be expressed by the

chemical potentials. For a neutral native vacancy, the formation energy can be defined as follows:[27]

$$E_f = (E_{tot}^v - E_{tot}^0 + n_i \mu_i)/n_i, \tag{1}$$

where E_{tot}^v and E_{tot}^0 are the total energies of the supercells with and without vacancies, n_i is the number of the atoms removed, and μ_i is the chemical potential of the corresponding atom, respectively. For example, the formation of a neutral oxygen vacancy requires the removal of one oxygen atom and the formation energy is given by

$$E_f(V_O) = E_{tot}^v(V_O) - E_{tot}^0(MgO) + \mu_O. \tag{2}$$

In thermodynamic equilibrium, the Mg and O chemical potentials satisfy the equation

$$\mu_{Mg} + \mu_O = \mu_{MgO}. \tag{3}$$

Here, μ_{MgO} is the chemical potential of MgO bulk. Under extreme O-rich condition, μ_O is subject to an upper bound given by the energy of O in an O_2 molecule ($\mu_O^{max} = \frac{1}{2}\mu_{O_2}$). Correspondingly, μ_{Mg} is derived from the relation

$$\mu_{Mg}^{min} = \mu_{MgO} - \frac{1}{2}\mu_{O_2}. \tag{4}$$

Under extreme Mg-rich condition, μ_{Mg} is subject to an upper bound given by the energy of Mg in bulk magnesium ($\mu_{Mg}^{max} = \mu_{Mg}^0$). Correspondingly, the upper limit on the magnesium chemical potential then results in a lower limit on the oxygen chemical potential

$$\mu_O^{min} = \mu_{MgO} - \mu_{Mg}^0. \tag{5}$$

The host chemical potentials thus vary over a range corresponding to the chemical potential of MgO bulk. In this paper, only the formation energies under extreme O-rich condition are considered.

III. RESULTS

A. Magnetism in MgO bulk

For a system to be magnetic, local magnetic moments should exist. To find the origin of the local magnetic moments, first, the electronic and magnetic properties are studied in perfect MgO bulk. The MgO bulk was modeled by a $(2 \times 2 \times 2)$ supercell, which contains 32 Mg and 32 O atoms. Perfect MgO normally crystallizes in the cubic rock salt structure, in which the cations are surrounded by octahedral anions with filled valence p bands. The Mg is in a 2+ state due to the donation of its two electrons to the neighbor O atom, which is in a 2− state. Perfect MgO is a nonmagnetic and wide band-gap material, where all bands are occupied. The calculated band gap is 4.7 eV, which is smaller than the experimental value[28] of 7.8 eV due to the DFT error of calculating band gap. The total DOS of perfect MgO is shown in Fig. 1(a). It is clear that the DOS of perfect MgO is identical for both projections of spin. The valence band is mainly composed of O 2p orbital and is full [Fig. 1(d)], whereas the conduction band is formed mainly by Mg 3s orbital (not shown) and is empty. The total magnetic moment of the sys-
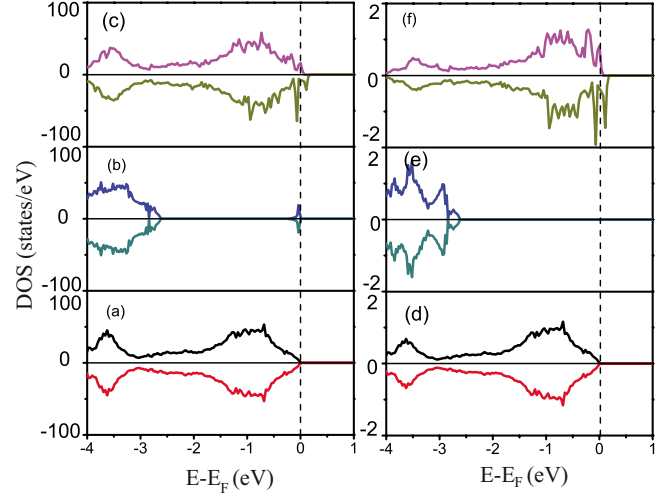
FIG. 1. (Color online) Total DOS and O 2p partial DOS of (a,d) the perfect MgO crystal ($Mg_{32}O_{32}$); (b,e) MgO bulk with one O vacancy ($Mg_{32}O_{31}$); (c,f) MgO bulk with one Mg vacancy ($Mg_{31}O_{32}$). In (b,e) and (c,f), the vertical dashed lines represent the Fermi energy, which is set to zero.

tem is zero. Now, at this point, local magnetic moments cannot form in perfect MgO.

Generally, there are two kinds of possible native point vacancies in MgO, which are magnesium vacancy (V_{Mg}) and oxygen vacancy (V_O). Though the charge states of the native vacancies in MgO can be 0, ±1, ±2, only the neutral native vacancies are considered in this paper. In order to study the effect of oxygen vacancies on the magnetic properties of MgO, one oxygen atom was removed to form an oxygen vacancy (V_O) in the $Mg_{32}O_{31}$ supercell. This led to O vacancy concentration of 3.125%. After full relaxation, the six nearest Mg atoms move outward slightly by only 0.01 Å with respect to the vacancy site. The total DOS and O 2p partial DOS of $Mg_{32}O_{31}$ supercell with one O vacancy are shown in Figs. 1(b) and 1(e), respectively. In the presence of O vacancy, the DOS remains spin unpolarized and the total magnetic moment of the system is zero. Generally, one O vacancy as a donor can introduce two electrons to the system and the Fermi energy shifts to higher energy. An impurity state of O vacancy appears in the band gap of MgO, which does not destroy the insulating behavior but decreases the band gap. The formation energy of O vacancy is calculated to be 7.00 eV. To study the effect of O vacancies concentration, two and three O atoms were also removed in the supercell. The corresponding concentrations of O vacancies are 6.25% and 9.375%, respectively. None of the system exhibits local magnetic moments, which suggests that O vacancies do not lead to magnetism in MgO independent of the concentration.

Next, one magnesium vacancy (V_{Mg}) was generated by removing one Mg atom in the $Mg_{31}O_{32}$ supercell, which corresponds to the concentration of 3.125%. As the nominal valence of Mg in perfect MgO is 2+, two holes are needed to charge compensate for a Mg vacancy. Because the neutral Mg vacancy has an open shell, it can lead to a spin-triplet state, which was found to be the ground state in MgO based on the experimental results.[29] After relaxation, the nearest O
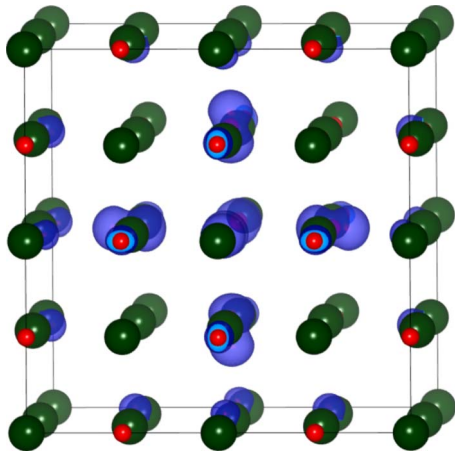
FIG. 2. (Color online) The isosurface plot of the spin density of $Mg_{31}O_{32}$ supercell with one Mg vacancy. The red small spheres represent O atoms, the large green spheres represent Mg atoms, and the blue isosurface shows the spin density, respectively.

FIG. 3. (Color online) (A) The relative energy of different configurations (I-V) as a function of the distance between two Mg vacancies. The zero in the vertical axis corresponds to the total energy (E_0) of configuration II (4.211 Å). (B) The energy difference between antiferromagnetic and ferromagnetic states as a function of the distance between two Mg vacancies.

atoms move outward as expected by almost 0.11 Å, while the second nearest Mg atoms move inward by about 0.07 Å. Unlike O vacancies, the presence of Mg vacancies leads to formation of local moments in the system. Basically, one Mg vacancy as an acceptor can leave two holes in the system and the calculated total magnetic moments before and after relaxation are 2.00 and 1.51 μ_B, respectively. The decrease in the magnetic moment is due to the large outward relaxation of the nearest neighbor O atoms. The main contribution to the total magnetic moment arises from the $2p$ orbitals of the six nearest octahedral O atoms to the vacancy, while the magnetic moments on Mg atoms are almost negligible. To visualize the changes in the electronic structure and magnetic properties resulting from Mg vacancies, the total DOS and O $2p$ partial DOS are shown in Figs. 1(c) and 1(f), respectively. Compared to the nonmagnetic perfect MgO, the Fermi energy moves to lower energy with holes existing at the top of the valence band. These new states result in an asymmetric spin-up and spin-down DOS near the Fermi energy. As shown in Fig. 1(f), the local moments in MgO mainly come from the spin polarization of O $2p$ orbitals. The strong spin polarization can also be visualized by plotting the defect states spin density in the real space. Figure 2 shows an isosurface plot of the spin density of $Mg_{31}O_{32}$ supercell. It is evident that the spin polarization is strongly localized near the six oxygen atoms surrounding the Mg vacancy. It is this localized spin polarization that leads to the formation of the local magnetic moments in the system.

However, the formation of localized magnetic moments does not necessarily lead to the collective magnetism. To promote magnetism, a minimum defects concentration needed for magnetic percolation should be granted.[16] The formation energy of Mg vacancy is 2.73 eV, which is much smaller than that of O vacancy. Thus, Mg vacancies can be generated more easily than O vacancies under O-rich condition during the growth process. Then the effect of Mg vacancies on the magnetism of MgO is also investigated by generating two and three Mg vacancies in the supercell. The corresponding concentrations of Mg vacancies are 6.25%

and 9.375%, respectively. For both cases, the spin polarization is obtained. The calculated total magnetic moments are 3.24 and 4.70 μ_B, respectively. It is shown that the total magnetic moment increases as the concentration of Mg vacancies increases. Thus, the presence of Mg vacancies leads to the spin polarization of O $2p$ orbitals and formation of local moments.

Do these vacancies-induced magnetic moments couple ferromagnetically or antiferromagnetically? Since the V_{Mg} defect leads to a partially occupied orbital at the Fermi energy [Fig. 1(c)], the interaction between two Mg vacancies could lower the total energy if the spins are arranged ferromagnetically.[30] To study the ferromagnetic interaction, two Mg vacancies were created in the supercell with all the atoms relaxed. The distance between the vacancies was varied and the total energies of the ferromagnetic and antiferromagnetic states were calculated. The line A in Fig. 3 shows the relative total energies of different configurations (I-V) as a function of V_{Mg} separation distance. It can be seen that the two Mg vacancies tend to form at the second nearest sites where the distance between them is 4.211 Å (configuration II). The energy difference ΔE between the antiferromagnetic and ferromagnetic states ($\Delta E = E_{AFM}\text{-}E_{FM}$) is used to study the stability of the ferromagnetic vs antiferromagnetic order of the two Mg vacancies. The energy difference ΔE as a function of the separation distance between two Mg vacancies is also shown in Fig. 3 (line B). As for the V_{Mg}-V_{Mg} interaction, the ferromagnetic order is found to be more favorable in most cases, although the distance certainly affects the stability of the ferromagnetic state. Since the percolation threshold concentration of the defects decreases clearly with the range of the ferromagnetic interaction increasing,[16] a long-range magnetic coupling is critical for achieving high temperature magnetism at low defect concentrations.[31] For MgO, the total energy of the ferromagnetic state is lower than that of the antiferromagnetic state even if the distance of the two Mg vacancies is 7.294 Å (configuration V). This indicates that a long-range ferromagnetic coupling may exist in the system to promote the collective magnetism. However,
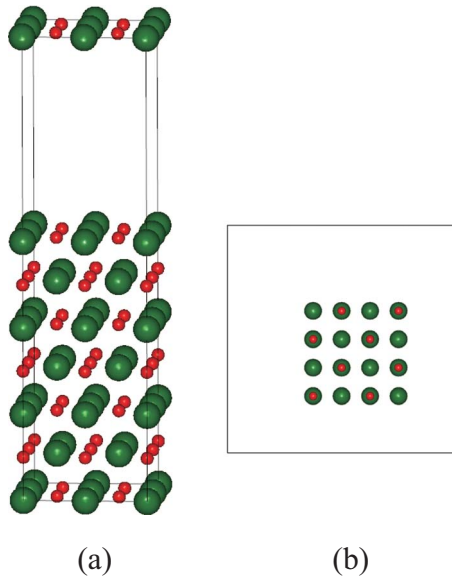
FIG. 4. (Color online) (a) A (2×2) seven-layer slab having (001) surface orientation. The vacuum region is 10 Å along the c direction. (b) MgO quantum dot supercell with vacuum space of 10.528 Å in each direction. The small red balls represent O atoms and the large green balls represent Mg atoms.

it should be noted that when the two Mg vacancies are separated by 5.158 Å (configuration III), the magnetic coupling between the local moments is vanishing ($\Delta E=0$). For configuration II with the lowest energy, the ferromagnetic state is only 28 meV lower in energy than the antiferromagnetic state. This value is smaller than the thermal energy (~ 30 meV) that corresponds to the room temperature. On one hand, the Mg vacancies-induced local magnetic moments may lead to long-range ferromagnetic interaction which depends on the spatial extend and symmetry of the interacting states.[30] On the other hand, the ferromagnetic state is not stable enough in bulk MgO at room temperature, which is consistent with the experimental result of diamagnetism in bulk MgO.

B. Magnetism in MgO thin films

To study the effect of surface defects on the electronic properties and magnetism of MgO, calculations were also carried out on MgO thin films. The MgO thin film was modeled by a (2×2) seven-layer slab having (001) surface orientation [Fig. 4(a)], which contains 28 Mg and 28 O atoms. Each slab was separated from the other by a vacuum region of 10 Å along the c direction. The central three layers of the slab were held at the bulk position, while the two layers on either side were taken to be identical to preserve symmetry and allowed to relax. The surface reconstruction was carried out by optimizing the structure using a $4\times4\times1$ Monkhorst-Pack k-point mesh.[25] For the DOS calculations of MgO slab, $5\times5\times2$ k mesh was used.

First, one oxygen vacancy was created by removing a single O atom from the surface layer of the slab. To preserve the symmetry, the corresponding O atom on the opposite side of the slab was also removed. This led to a $Mg_{28}O_{26}$ super-
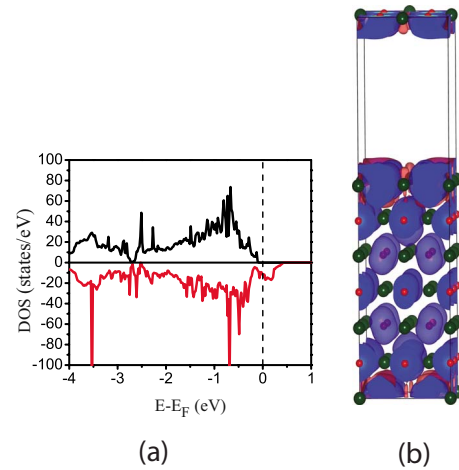
FIG. 5. (Color online) (a) Total DOS of MgO (001) slab with two surface Mg vacancies in either side. The vertical dashed lines represent the Fermi energy which is set to zero. (b) The spin density of MgO (001) slab with two surface Mg vacancies in either side. The red small spheres represent O atoms, the large green spheres represent Mg atoms, the blue and wine isosurfaces show the up and down spin densities, respectively.

cell with O vacancies concentration of 7.1%. For O vacancy at the surface site, the formation energy is found to be 6.38 eV, which is smaller than that in the bulk. To see whether O vacancy tends to locate on the subsurface layer, one O atom was also removed from the subsurface layer on either side of the slab. Since the two vacancies in the top and bottom subsurface layers of the slab are far apart (8.422 Å), the interaction between them is very small. The corresponding formation energy of the subsurface O vacancy is calculated to be 6.89 eV, which is larger than that of the surface O vacancy. Thus, the formation of O vacancies is easier on the surface layer than on the subsurface layer or in the bulk. As in the bulk, the spin polarized calculations show that O vacancy induces no magnetism in MgO thin films irrespective of its site.

Second, the effect of Mg vacancies on the magnetism of MgO thin films is studied by generating one Mg vacancy on each side of the surface and subsurface layers in the supercell, respectively. For both cases, the system exhibits local magnetic moments when introducing Mg vacancies. The total DOS of MgO slab with Mg vacancies in the surface layer is shown in Fig. 5(a). It is clear that Mg vacancies introduce spin polarization near the Fermi energy. The total magnetic moment of the system with surface Mg vacancies is 4.00 μ_B, which implies that each Mg vacancy can induce a moment of 2.00 μ_B. The main contribution to the magnetic moment comes from the five nearest O atoms [Fig. 5(b)]. On the (001) surface, each Mg atom directly binds with five O atoms, in which four of them are on the surface layer while the other one resides in the subsurface layer. Each of the surface O atoms has a magnetic moment of 0.33 μ_B while the moment on the subsurface O atom is 0.14 μ_B. As shown in Fig. 5(b), the remaining magnetic moments mainly reside on the O atoms of the central three layers. When Mg vacancies locate on the subsurface layer, the induced total magnetic moment is also 4.00 μ_B, which mainly arises from the

$2p$ orbitals of the nearest O atoms. Each of the four equatorial O atoms on the subsurface layer has the largest moment of 0.23 μ_B, while the two apical O atoms on the surface and the third layers carry magnetic moments of 0.18 and 0.19 μ_B, respectively. The formation energies of Mg vacancies on the surface and the subsurface layers are 2.45 and 2.74 eV, respectively. It is noted that like anion vacancy, the cation vacancy tends to form at the surface site than at the subsurface or in the bulk, which is similar as that in GaN.[32] This phenomenon occurs because there is less number of bonds that need to be broken on the surface than in the subsurface layer.[10] Thus, a large concentration of Mg vacancies may form at the surface or the region near the surface, which can introduce local moments in MgO.

C. Magnetism in MgO quantum dot

As the ferromagnetism was found in MgO nanocrystals (24–52 nm) while the bulk MgO showing diamagnetism, the dimension and quantum confinement effects may play an important role on the defect-induced magnetism, so that further calculations have also been carried out on MgO quantum dot. The quantum dot was constructed from a $(4 \times 4 \times 4)$ MgO supercell by removing the surrounded magnesium and oxygen atoms and replacing them with a vacuum space [Fig. 4(b)]. Thus, the corresponding supercell contains 32 f.u. of MgO and the vacuum space is 10.528 Å. In order to improve the precision, $4 \times 4 \times 4$ Monkhorst-Pack k mesh[25] was used for the calculations. The size in the diagonal direction of the quantum dot is about 11 Å.

Again, one Mg atom was removed in the supercell to study the magnetism of MgO quantum dot. As in the bulk and thin films, each Mg vacancy can introduce two holes to the system and the corresponding magnetic moment of the system is 2.00 μ_B. It can be seen from the total DOS of MgO quantum dot that clear exchange spin splitting appears near the Fermi energy [Fig. 6(a)]. The isosurface of the spin density is plotted in Fig. 6(b). This shows that the total magnetic moments mainly arise from the up-spin density residing on the O atoms. There is a little down-spin density distributing in the interatomic region and on the magnesium atoms. Thus, the origin of the defect-induced magnetism is related to the existence of $2p$ holes of well-defined spin polarization at the valence band. According to the Stoner Criterion,[33] spontaneous ferromagnetism can occur if it satisfies $D(E_F)J > 1$. Here, $D(E_F)$ is the DOS at the Fermi energy E_F and J denotes the strength of the exchange interaction. It has been proved that first row element O has very large exchange interaction J for the $2p$ orbitals which are localized with large effective masses m due to the high ionicity.[12] Because the density of states at the Fermi energy $D(E_F)$ is proportional to $m^{3/2}\sqrt{E_{VBM} - E_F}$,[12] if more holes are introduced, the Fermi energy E_F would move deep into the valence band and lead to a large DOS at E_F. Since the formation energy of Mg vacancy in the quantum dot (1.37 eV) is much smaller than that in the bulk and thin films, a larger concentration of Mg vacancies can form in the quantum dot. This leads to a large concentration of holes in the top of the valence band. Furthermore, the localized nature (large effective masses m) of
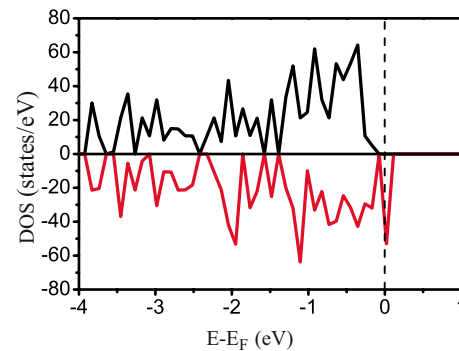
(a)
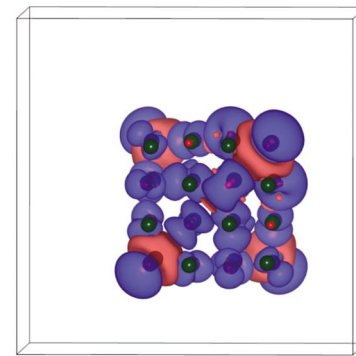
(b)

FIG. 6. (Color online) (a) Total DOS of MgO quantum dot with one Mg vacancy. The vertical dashed lines represent the Fermi energy which is set to zero. (b) The spin density of MgO quantum dot with one Mg vacancy. The red small spheres represent O atoms, the large green spheres represent Mg atoms, and the blue and wine isosurfaces show the up and down-spin densities, respectively.

the $2p$ states of O atom and quantum confinement effects may also lead to a large DOS at the Fermi energy [Fig. 6(a)]. Thus, magnetization can be sustained in low dimensional MgO quantum dot when enough holes are introduced by large concentration of Mg vacancies. This agrees with the experimental result of ferromagnetism observed in the nanocrystals.

IV. DISCUSSIONS

As mentioned above, one Mg vacancy as an acceptor leaves two holes in the system and leads to formation of local magnetic moments. The origin of the local moments can be understood from the energy levels and occupation of the defect states. In perfect MgO, the Mg cations are surrounded by an octahedron of six O anions with filled valence p bands. The symmetry of this octahedral crystal field is O_h. According to the molecular orbital theory (MOT), the linear combination of the atomic orbitals of the central metal and the σ-type orbitals of the six ligands forms the σ-bonding molecular orbitals. The symmetries of these molecular orbitals are a_{1g}, t_{1u}, and e_g. In the crystal field of O_h symmetry, the highest energy levels for electrons (the lowest energy levels for holes) are the doubly degenerate e_g orbitals, which
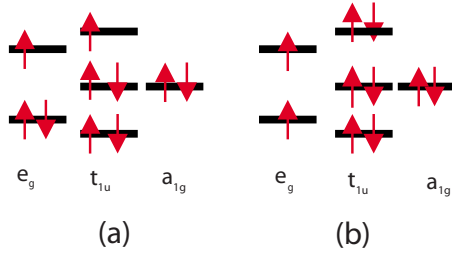
FIG. 7. (Color online) The schematic occupation diagram of the molecular orbitals in MgO with one Mg vacancy. The red vertical arrows represent the occupied electrons with up or down spins. (a) One electron is transferred from t_{1u} orbitals to e_g orbitals. (b) There is no charge transfer between the orbitals with different symmetries.

are fully occupied. Since two electrons are removed due to the charge compensating effect in the presence of Mg vacancy, the highest occupied molecular orbitals (HOMO) for electrons (e_g) are partially occupied. Similar to the case of CaO, the exchange interaction further leads to the splitting of the spin-up and spin-down channels and there may be some electron density transferred from t_{1u-} orbitals to e_{g-} orbitals.[16] Therefore, the electronic configuration of the defect complex $V_{Mg}^0 O_6^{10-}$ is $(a_{1g}^2 t_{1u+}^3 e_{g+}^2) t_{1u}^p e_{g-}^q$ ($p+q=3$). Thus, the net spin of the whole system is S$=[(3-p)+(2-q)]/2$ $=1$, which leads to a spin-triplet state. As schematically illustrated in Fig. 7(a), the neutral Mg vacancy leads to a spin triplet with a net magnetic moment of 2.0 μ_B (assuming $p=2$, $q=1$). In this case, one hole is located in e_g orbitals while the other in t_{1u} orbitals. If there is no electron density transferred from t_{1u-} orbitals to e_{g-} orbitals ($p=3$, $q=0$), i.e., both holes are located in parallel in e_g orbitals according to the Hund's rules, the defect state is also in a spin-triplet state [Fig. 7(b)].

To investigate the mechanism of the exchange interaction between the local magnetic moments, the isosurface plots of spin density of the configuration IV with the largest energy difference ΔE are shown in Figs. 8(a) and 8(b). The spin polarization shows clearly not only localized nature with most of the spin density on the surrounded oxygen atoms neighbor to the vacancy but extended nature with the spin density extended to almost the whole supercell. The up-spin density mainly localizes on the oxygen atoms while the down-spin density mainly in the interatomic zone and on the magnesium atoms. Thus, the spin polarization of the defect states overlaps with each other which may mediate the long-range magnetic coupling. This duality (localization vs extension) opens up the possibility of the long-range magnetic coupling between the defect-induced local moments.[31] The ferromagnetic coupling between the vacancy induced local magnetic moments can be explained by the through-bond spin polarization mechanism.[34] The up-spin density mainly residing on the oxygen atoms induces a down-spin density in the interatomic zone and on the adjacent magnesium atom along the O–Mg bond direction. Thus, the through-bond spin polarization takes place along the O-Mg-(O-Mg)$_n$-O (n $=0,1,2,\cdots$) path [Fig. 8(c)]. Since the number of the O–Mg bonds in this path is even, the up-spin densities on the oxygen atoms couple ferromagnetically.[35] Therefore, it is indi-
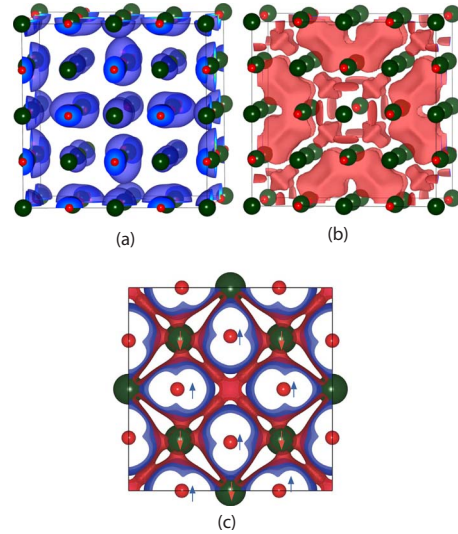
FIG. 8. (Color online) The up (a) and down (b) spin densities of bulk MgO supercell with two Mg vacancies (configuration IV). (c) Illustration of the mechanism of through-bond spin polarization and the spin density of the section with the two Mg vacancies in configuration IV of bulk MgO. The red small spheres represent O atoms, the large green spheres represent Mg atoms, and the blue and wine isosurfaces show the up and down-spin densities, respectively.

cated that the through-bond spin polarization mechanism mediates the ferromagnetism in MgO.

V. SUMMARY

In summary, the electronic and magnetic properties of MgO bulk, thin films and quantum dot have been studied by density functional theory calculations. The results show that O vacancies do not lead to magnetism in MgO independent of the concentration. Nevertheless, spin polarization appears at the top of the valence band when introducing Mg vacancies. The local magnetic moments mainly arise from the 2p orbitals of the nearest O atoms. The partially occupied e_{g-} and t_{1u-} (or only e_{g-}) orbitals lead to a local magnetic moment in the system and the through-bond spin polarization mediates the ferromagnetism in MgO. For bulk MgO with Mg vacancies in the ground state configuration II, the energy difference between the antiferromagnetic and ferromagnetic states is only 28 meV, which is not large enough against the thermal fluctuations at room temperature. This is consistent with the experimental result of no FM in bulk MgO. In MgO thin films, the formation energy of Mg vacancy at the surface site is lower than that at the subsurface site or in the bulk, which indicates Mg vacancies tend to form at the surface or the region near the surface. In the case of MgO quantum dot, the formation energy of Mg vacancy decreases much with the dimension of the system decreasing and a larger concentration of Mg vacancies expectedly appearing. In conclusion, the magnetism can be sustained in the quantum dot when enough holes introduced by the large concentration of Mg vacancies, which is consistent with the experimental result of magnetism observed in MgO nanocrystals.

*Author to whom correspondence should be addressed; hansh@sdu.edu.cn

[1] T. Dietl, H. Ohno, F. Matsukura, J. Cibert, and D. Ferrand, Science **287**, 1019 (2000).

[2] T. Jungwirth, J. Sinova, J. Mašek, J. Kušera, and A. H. MacDonald, Rev. Mod. Phys. **78**, 809 (2006).

[3] M. Venkatesan, C. B. Fitzgerald, and J. M. D. Coey, Nature (London) **430**, 630 (2004).

[4] J. M. D. Coey, Solid State Sci. **7**, 660 (2005).

[5] C. Das Pemmaraju and S. Sanvito, Phys. Rev. Lett. **94**, 217205 (2005).

[6] J. M. D. Coey, M. Venkatesan, P. Stamenov, C. B. Fitzgerald, and L. S. Dorneles, Phys. Rev. B **72**, 024450 (2005).

[7] N. H. Hong, J. Sakai, N. Poirot, and V. Brizé, Phys. Rev. B **73**, 132404 (2006).

[8] A. Sundaresan, R. Bhargavi, N. Rangarajan, U. Siddesh, and C. N. R. Rao, Phys. Rev. B **74**, 161306(R) (2006).

[9] H. Peng, J. Li, Shu-Shen Li, and Jian-Bai Xia, Phys. Rev. B **79**, 092411 (2009).

[10] Q. Wang, Q. Sun, G. Chen, Y. Kawazoe, and P. Jena, Phys. Rev. B **77**, 205411 (2008).

[11] Xu Zuo, Soack-Dae Yoon, Aria Yang, Wen-Hui Duan, Carmine Vittoria, and Vincent G. Harris, J. Appl. Phys. **105**, 07C508 (2009).

[12] Haowei Peng, H. J. Xiang, Su-Huai Wei, Shu-Shen Li, Jian-Bai Xia, and Jingbo Li, Phys. Rev. Lett. **102**, 017201 (2009).

[13] G. Rahman, V. M. García-Suárez, and S. C. Hong, Phys. Rev. B **78**, 184404 (2008).

[14] Xiaoping Han, Jaichan Lee, and Han-Ill Yoo, Phys. Rev. B **79**, 100403(R) (2009).

[15] I. S. Elfimov, S. Yunoki, and G. A. Sawatzky, Phys. Rev. Lett. **89**, 216403 (2002).

[16] J. Osorio-Guillén, S. Lany, S. V. Barabash, and A. Zunger, Phys. Rev. Lett. **96**, 107203 (2006).

[17] S. Gallego, J. I. Beltrán, J. Ceradá, and M. C. Muñoz, J. Phys.: Condens. Matter **17**, L451 (2005).

[18] J. Hu, Z. Zhang, M. Zhao, H. Qin, and M. Jiang, Appl. Phys. Lett. **93**, 192503 (2008).

[19] W. Kohn and L. J. Sham, Phys. Rev. **140**, A1133 (1965).

[20] G. Kresse and D. Joubert, Phys. Rev. B **59**, 1758 (1999).

[21] J. P. Perdew and Y. Wang, Phys. Rev. B **33**, 8800 (1986).

[22] J. P. Perdew, K. Burke, and M. Ernzerhof, Phys. Rev. Lett. **77**, 3865 (1996).

[23] G. Kresse and J. Furthmüller, Phys. Rev. B **54**, 11169 (1996).

[24] G. Kresse and J. Furthmüller, Comput. Mater. Sci. **6**, 15 (1996).

[25] H. J. Monkhorst and J. D. Pack, Phys. Rev. B **13**, 5188 (1976).

[26] D. Taylor, Br. Ceram. Trans. J. **83**, 5 (1984).

[27] A. Janotti and C. G. Van de Walle, Phys. Rev. B **76**, 165202 (2007).

[28] R. C. Whited, C. J. Flaten, and W. C. Walker, Solid State Commun. **13**, 1903 (1973).

[29] B. H. Rose and L. E. Halliburton, J. Phys. C **7**, 3981 (1974).

[30] P. Mahadevan, A. Zunger, and D. D. Sarma, Phys. Rev. Lett. **93**, 177201 (2004).

[31] P. Dev, Y. Xue, and P. Zhang, Phys. Rev. Lett. **100**, 117204 (2008).

[32] Z. Wang, B. Huang, L. Yu, Y. Dai, P. Wang, X. Qin, Xiaoyang Zhang, Jiyong Wei, Jie Zhan, Xiangyang Jing, Haixia Liu, and Myung-Hwan Whangbo, J. Am. Chem. Soc. **130**, 16366 (2008).

[33] E. C. Stoner, Proc. R. Soc. London, Ser. A **165**, 372 (1938); **169**, 339 (1939).

[34] K. Yoshizawa, T. Kuga, T. Sato, M. Hatanaka, K. Tanaka, and T. Yamabe, Bull. Chem. Soc. Jpn. **69**, 3443 (1996).

[35] H. Jin, Y. Dai, BaiBiao Huang, and M.-H. Whangbo, Appl. Phys. Lett. **94**, 162505 (2009).